ChemComm

Accepted Manuscript

This article can be cited before page numbers have been issued, to do this please use: R. Ahmad, N. Tripathy, J. Park and Y. Hahn, *Chem. Commun.*, 2015, DOI: 10.1039/C5CC03656A.

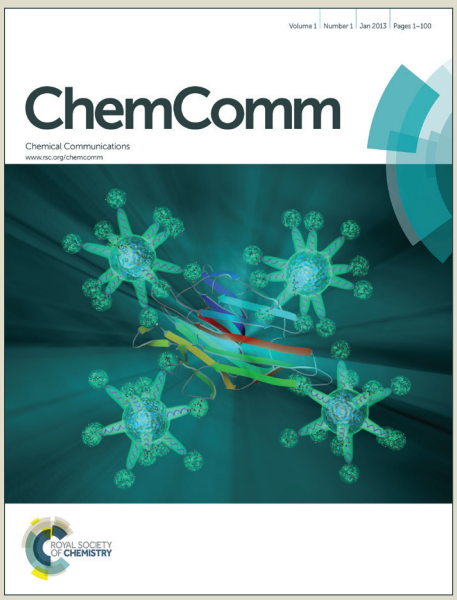

ROYAL SOCIETY OF CHEMISTRY

www.rsc.org/chemcomm

View Article Online
DOI: 10.1039/C5CC03656A

ChemComm

COMMUNICATION

Comprehensive biosensor integrated with ZnO nanorods FETs array for selective detection of glucose, cholesterol and urea†

Received 00th January 20xx,
Accepted 00th January 20xx

DOI: 10.1039/x0xx00000x

www.rsc.org/

Rafiq Ahmad,[a] Nirmalya Tripathy,[b] Jin-Ho Park[c] and Yoon-Bong Hahn[a,*]

We report a novel straightforward approach for simultaneous and highly-selective detection of multi-analyte (i.e. glucose, cholesterol and urea) with integrated field-effect transistors (i-FETs) array biosensor without any interference in each sensor response. Compared to analytically-measured data, performance of the ZnO nanorods based i-FETs array biosensor is found to be highly reliable for rapid detection of multi-analytes in mice blood, serum and blood samples of diabetic dogs.

Nanotechnology revolution has led to the nanofabrication of sensor devices for rapid and specific identification of chemical/biological species. However, the development of multiplexed nanoscale biosensor for simultaneous detection of different analytes still remains a major challenge at the nanotechnology frontier. It is well recognized that diabetes mellitus is a metabolic disorder resulting in an abnormal blood glucose level and activation of several metabolic pathways related to inflammation and apoptosis events.[1] According to World Health Organization, approximately 3.4 million people died from high blood sugar in 2004 and diabetes will be the 7th leading cause of death in 2030.[2] Cholesterol, another important biomolecule, with increased level in blood can lead to heart diseases, stroke, coronary artery disease, arteriosclerosis, cerebral thrombosis, etc.[3] Overall, raised cholesterol is estimated to cause 2.6 million deaths (4.5% of total) and 29.7 million disability adjusted life years. On the other hand, urea in serum/blood/urine is important for diagnosis of renal and liver diseases.[4] To date, a plethora of advanced biosensor designs were proposed for the selective detection of single analyte in blood for diagnosis, and management of several diseases.[5] Emphasizing on human health and clinical use point of view, there is urgent requirement for the development of biosensor devices capable of simultaneous detection of clinically important biomolecules coupled with high sensitivity, excellent selectivity, fast response and cost-effective.

FETs utilizing nanorods or nanowires are particularly impressive, robust and economically feasible platforms to achieve high current amplification and sustaining an enhanced signal-to-noise ratio among all the detection methodologies owing to their excellent sensitivity, label-free, real-time response for bio- and chemical molecules detection.[6] Sensing performances of enzymatic sensors are greatly affected by the immobilized enzyme quantity onto the engineered nanostructure.[7] Thus, directly grown vertical nanorods were found to be the most promising for designing sensor devices due to its large surface area, good attachment features, high enzyme immobilization efficiencies, bioactivity retainment, etc. Zinc oxide nanorods (ZnO NRs) has received enormous attention for efficient electrode and device fabrication, drug delivery, biomedical applications, so on.[9]

In this communication, inspired by the nanostructure and material benefits, for the first time we report a novel straightforward approach for simultaneous detection of multi-analyte (i.e. glucose, cholesterol and urea) with ZnO NRs based i-FETs array biosensor. Key to our sensor design is an integrated approach capable of selective and simultaneous detection of biomolecules on three different FETs without any interference in each sensor response.

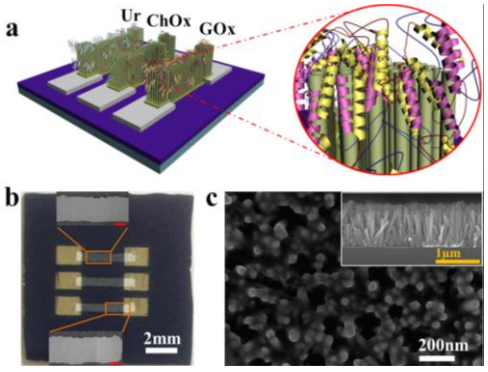

Fig. 1 (a) Schematic of ZnO NRs i-FETs array biosensor with immobilized enzymes and a zoom-in view. (b) Optical image of i-FETs array biosensor showing three ZnO NRs arrays and FESEM images of their selected area (scale bar = 500 μm). (FESEM top- and cross-sectional (inset) images of ZnO NRs after and before enzyme immobilization, respectively.

[a] School of Semiconductor and Chemical Engineering, Nanomaterials Processing Research, Chonbuk National University, 567 Baekje-daero, Deokjin-gu, Jeonju 561-756, Republic of Korea. E-mail: ybhahn@chonbuk.ac.kr
[b] Department of BIN Fusion Technology, Chonbuk National University, 567 Baekje-daero, Deokjin-gu, Jeonju 561-756, Republic of Korea
[c] Department of Veterinary Internal Medicine, College of Veterinary Medicine, Chonbuk National University, 567 Baekje-daero, Deokjin-gu, Jeonju 561-756, Republic of Korea

† Electronic Supplementary Information (ESI) available: Experimental details, electrical properties, blood samples analysis. See DOI: 10.1039/x0xx00000x

Further, the i-FETs biosensor feasibility was assessed in mice and dog blood samples (normal, hypo- and hyper-glycemic).

Details of experimental and fabrication processes of ZnO NRs i-FETs array biosensor are shown in ESI (Fig. S1). Fig. 1 shows the schematic illustration of ZnO NRs i-FETs array biosensor after enzymes immobilization (a) and the optical image of biosensor showing ZnO NRs FETs array having channel length and width of 5 and 2 mm, respectively (b). Vertically aligned and uniform ZnO NRs are grown on patterned areas with well-defined gap between the FETs. The FESEM image (top and bottom insets) in Fig. 1b illustrates high degree of ZnO NRs uniformity over the patterned areas. The ZnO NRs arrays density and uniformity are further confirmed by the top- and cross-sectional FESEM views (Fig. 1c). The top view taken after enzymes immobilization, clearly displays the abundance and even immobilization of enzymes on the ZnO NRs surfaces. The crystallinity and crystal phase of ZnO NRs are characterized by TEM and XRD, respectively (Fig. S2, ESI).

The electrical properties of ZnO NRs i-FETs array before and after enzymes immobilization on ZnO NRs (Fig. S3a-c, ESI) shows an Ohmic contact and confirm that the enzyme molecules are effectively immobilized on the ZnO NRs without any deterioration in electrical contact and conductivity. Compared to the I-V plots for ZnO NRs on seed layer, the conductivity of seed layer (Fig. S3d, ESI) is almost negligible (pA level). Hence, it is concluded that the entire conductance change originates only from the NRs after enzymatic reactions. The consensus is also supported by our previous work based on the ZnO NRs applications for amperometric sensor for cholesterol detection; high enzyme immobilization on ZnO NRs leading to good electrocatalytic reactions and fast electron conduction through the NRs.[10]

Fig. 2a shows the ZnO NRs i-FETs biosensor set-up. All the experiments have been carried out after investigating the working potential range, pH change with increasing concentrations of glucose, cholesterol and urea, and pH effect on biosensor response (for details see Fig. S4-S6, ESI). Prior to the measurements of analytes in solution, the silver source-drain electrodes are passivated with PDMS, leaving active area for each sensor to reduce the leak current and eliminate the effect of metal-nanorods contact region, which ensures that the entire conductance changes originate only from the nanorods. Notably, the uniqueness of our sensor is that the ZnO NR itself acts as a good conduction pathway because of its high electron affinity. Thus, the electrons generated from enzymatic reactions on the surface of each nanorod pass directly through the nanorods to the seed layer to the electrode rather than in transverse direction. To study the response of the purposed solution-gated ZnO NRs i-FETs biosensor, the sensor response (I_D) is recorded with an optimized and constant bias potential range across the electrodes in the absence/presence of 1 mM of each glucose, cholesterol and urea in PBS solution. As shown in Fig. 2b-d, the current value substantially increases with analyte compared to that without it. This increase in current response is considered to be due to the enzymatic reactions of the respective enzymes with analyte in the presence of oxygen. The enzymatic reactions temporarily change the protonation state of conducting ZnO NRs and thus affect the I_D (drain current) with increasing V_G (gate voltage). The chemical reactions for enzymatic breakdown of

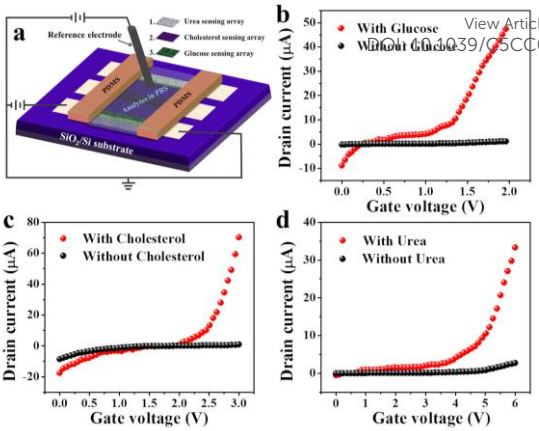

Fig. 2 (a) Side-view illustration of constructed ZnO NRs i-FETs array biosensor. (b-d) Typical I_D-V_G responses of ZnO NRs i-FETs array biosensor without and with 1 mM of each glucose, cholesterol and urea in 0.05 M PBS buffer.

glucose via GOx along with the subsequent oxidation of hydrogen peroxide (H_2O_2) are as follows:[11]

$$\text{Glucose} + O_2 \xrightarrow{\text{GOx}} \text{Gluconolactone} + H_2O_2 \quad (1)$$

$$H_2O_2 \rightarrow O_2 + 2H^+ + 2e^- \quad (2)$$

The GOx converts glucose into Gluconolactone and H_2O_2 through its reaction with the oxygen present in solution. The generated H_2O_2 can alter the charge transfer property of GOx-ZnO NR. Similarly, an enzymatic reaction of the ChOx produces H_2O_2 and at a suitable potential electro-oxidation current of H_2O_2 is detected. The possible mechanism of the enzymatic reaction catalyzed by ChOx is according to the following reaction.[12]

$$\text{Cholesterol} + O_2 \xrightarrow{\text{ChOx}} \text{Cholest-4-en-3-one} + H_2O_2 \quad (3)$$

$$H_2O_2 \rightarrow O_2 + 2H^+ + 2e^- \quad (4)$$

Moreover, enzymatic urea detection is generally based on determining the products of urea-based hydrolysis formed in accordance with the following reaction.[13]

$$H_2N\text{-}CO\text{-}NH_2 + 3H_2O \xrightarrow{\text{Urease}} 2NH_4^+ + HCO^{3-} + OH^- \quad (5)$$

As a result of this reaction one HCO^{3-} and two NH^{4+} ions produced from the uncharged urea. The ammonium ions react with the ZnO NRs and produce the current change of the biosensor.

To explore the sensing properties of the fabricated ZnO NRs i-FETs array biosensor, experiments have been conducted under optimal conditions. Simultaneously, the detection of glucose, cholesterol and urea has carried out on three different arrays and the I_D-V_G responses of the sensor are shown in Fig. 3a-c. It is evident that the current increases substantially with increasing the concentration of analyte at room temperature. This is attributed to an increase in ions concentrations and fast communication of electrons throughout the reaction. The noticeable current changes for glucose, cholesterol and urea are obtained based on concentrations at a higher potential range, i.e. 1.0-2.0, 2.0-3.0 and 4.5-6.0 V, respectively. The increase in current on these ranges are further considered for plotting the calibration curve of fabricated sensor current response *vs.* analyte concentrations (Fig. 3d), by taking average of currents over the range of potentials. The calibration plots after performing each experiment (three times) have been used for the calculation of sensitivity and linear range, which are the two vital indicators of sensing performance of any

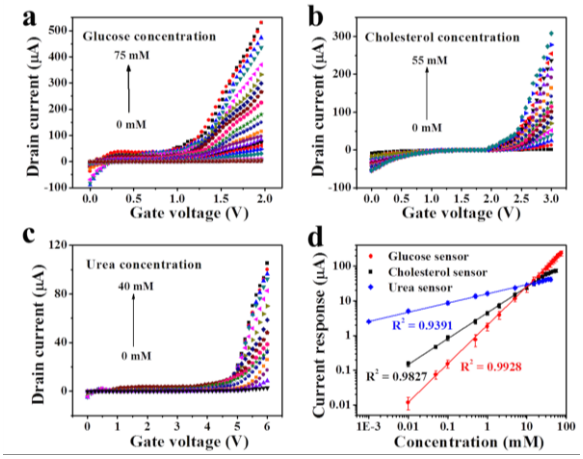

Fig. 3 I_D-V_G responses of ZnO NRs i-FETs array biosensor with increasing (a) glucose (0-75 mM), (b) cholesterol (0-55 mM) and (c) urea concentrations (0-40 mM) in 0.05 M PBS buffer. Their corresponding calibration plots (d) in log scale showing linearity with high regression coefficient.

sensor. The logarithmic plot of current response *vs.* analyte concentration yields a linear behavior in the concentration ranges of 0.05-70, 0.01-45 and 0.01-30 mM for glucose, cholesterol and urea, respectively with a high regression coefficient value, indicating a high degree of accuracy throughout the assay range. The fabricated i-FET biosensors show the high sensitivity of 32.27, 17.10 and 14.23 μA cm^{-2} mM^{-1} and low limit of detection of 0.07, 0.04 and 0.032 μM for glucose, cholesterol and urea, respectively, calculated from the slope of current-concentration plot (S) and the standard deviation of the response (SD). The ZnO NRs i-FET biosensor also showed good stability and reproducibility. The stability of sensor has been determined by repetitive measurements (50 cycles) and once a day for 8 weeks (Fig. S7 and S8, ESI). Overall, the sensor shows high stability for repetitive measurements and retains about 94 % of its original response after 50 times measurements and 40 days of storage for each analyte. The small decrease in response is probably due to the loss of immobilized enzyme or loss of bioactivity with repetitive use.

To verify the selectivity of ZnO NRs i-FETs array biosensor, interference test has been performed with mice whole blood, serum samples and PBS buffer (each containing glucose, cholesterol and urea in similar concentration). The blood samples used in the experiments are freshly drawn from normal mice followed by estimation of glucose, cholesterol and urea concentration (with no interfering species) using commercial estimation kits, shown in Fig. 4 as histogram. As compared with PBS sample, the concentrations of glucose, cholesterol and urea measured in filtered blood (serum sample) are almost similar, which suggests that the interfering species present in serum do not have any obvious effect on the performance of ZnO NRs i-FETs array biosensor. However, when the real blood of mice is used, there are slight decreases in biosensor response for glucose, cholesterol and urea, i.e. 7, 19, 12 %, respectively. This decline in the biosensor response is ascribed to the presence of different types of molecules (such as cells, protein fragments, etc.) in mice blood. These molecules restrict the diffusion of analyte into the immobilized enzyme thereby decrease the ZnO NRs i-FETs array based biosensor response. In order to further study the reusability, the used biosensors are removed from whole blood samples and tested in buffer solution. We observe that the biosensor recovered most of its response (~97 %) even after 20 times of washing, which shows its reliability for repeated usages.

In order to demonstrate the reliability of the ZnO NRs i-FETs array biosensor for routine analysis, the biosensor has been tested for the determination of glucose, cholesterol and urea concentrations in five freshly drawn mice whole blood samples. A slight decrease in the biosensor response for the analytes measured in mice whole blood, i.e. 7, 19, 12 % for glucose, cholesterol and urea, respectively (reason explained above) is noticed. Hence, in order to calculate the actual concentrations of analytes in mice whole blood samples, the obtained results of glucose, cholesterol and urea concentration are calibrated by adding 7, 19, 12 % to their respective values, because the device shows a decrease in response when directly used for the whole blood samples. Interestingly, we found that the finally calibrated values of analyte in all the whole blood samples are almost similar to the measured values using standard tools. The comparison results are displayed in Fig. S9 histogram and also listed in Supplementary Table S1, confirming that the ZnO NRs i-FETs array biosensor can be utilized for practical sample testing with favorable accuracy and precision. Moreover, the potential of ZnO NRs i-FETs array biosensor has also been demonstrated by determining analyte concentrations in diabetic dog patients. Collected blood samples from hypoglycemic (sample 1-10) and hyperglycemic (sample 11-21) dogs and filtered serum samples are used for the glucose, cholesterol and urea determination. The measured data are shown in ESI (Fig. S10), where all three analyte (glucose, cholesterol and urea) are directly detected in the serum samples without any further dilution. To validate the performance of ZnO NRs i-FET biosensor, the determined results are compared with those provided by the analytically measured values (Table S2). The values measured by the developed biosensor are in good agreement with the data obtained by the analytically measured. This agreement demonstrates the practical application of this high performance ZnO NRs i-FETs array biosensor for clinical glucose, cholesterol and urea detection. This not only provides the information of glucose, cholesterol and urea abnormalities but also yields a crucial indicator of liver and kidney malfunctions.

In summary, we developed a ZnO NRs i-FETs array biosensor

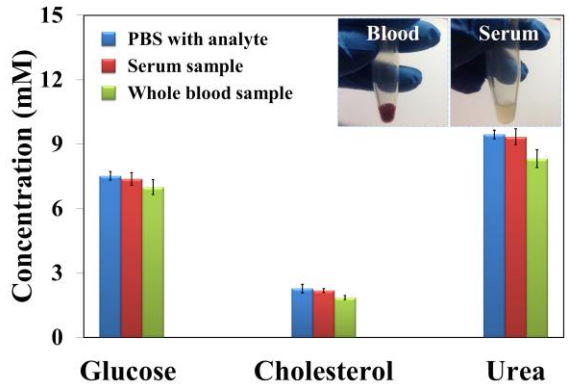

Fig. 4 Comparative results of the interference test in the mice whole blood and serum samples with PBS (0.05 M) buffer containing equal concentrations of glucose (7.6 mM), cholesterol (2.3 mM) and urea (9.5 mM) to those of blood and serum samples. Inset showing photo image of mice whole blood sample before and after filtration.

with simultaneously immobilizing GOx, ChOx and Ur enzymes on three different ZnO NRs arrays. The ZnO NRs i-FETs array biosensors provide fast responses towards wide linear ranges of glucose, cholesterol and urea with high sensitivities and low limit of detections. We experimentally observed that the i-FETs array biosensors show almost negligible interference in PBS and filtered serum samples, whereas a slight decrease in the response is evident for whole mice blood samples. Furthermore, the i-FETs array biosensors are successfully used for the determination of glucose, cholesterol and urea concentrations in whole mice blood samples. Impressively, the concentrations determined by the fabricated biosensor for glucose, cholesterol and urea (including the calculated interference caused during measurements) are well-matched with those of the pre-analytically determined. Thus, this approach has a great potential to become a useful tool not only for biomedical research but also for patients suffering from glucose, cholesterol, urea related disorders/diseases.

Although the obtained results are very interesting, the sensor array using an electrode still places certain limits on size and testing volume. Specifically, in this work, the sensor chip is advantageous for detection of analytes in wide linear ranges, which does not require samples dilution, thus making it ideal for clinical applications such as blood-based analytes measurements. On the other hand, the previously designed multi-analyte biosensors are mostly based on electrochemical techniques requiring potentiometry, amperometry, voltammetry, and electrochemical impedance spectroscopic measurements. Despite their widespread clinical use, these techniques have a number of potential limitations. For example, not all the protein analytes/samples are intrinsically capable to serve as redox partners in electrochemical reactions. Hence a suitable label must be introduced in order to promote the electrochemical reaction of the analyte at the working electrode for their detections. Moreover, these assays not only require samples dilution but also are quite expensive. However, for easy operation of these sensor chips in laboratories and at home or development of wearable and implantable device, the chip size should be reduced for real-time measurements. Noteworthy, using this FETs approach, we can also enhance the detection sensitivities by the use of amplification. The development of an integrated, low-cost ZnO NRs i-FETs array biosensors will produce quick detection under critical patient conditions, early identification of disease/disorder, and also have an enormous impact on the future generations.

This work was supported in part by the Ministry of Trade, Industry and Energy (Korea) and by the National Leading Research Laboratory program (2013064831) through the National Research Foundation (NRF) of Korea funded by the Ministry of Science, ICT & Future Planning. Authors also thank KBSI, Jeonju branch for SEM analysis and Mr. Jong-Gyun Kang, Center for University Research Facility (CURF) for taking good quality TEM images.

Notes and references

1 (a) S. K. Vashist, D. Zheng, K. Al-Rubeaan, J. H. T., Luong and F. S. Sheu, Anal. Chim. Acta, 2011, **703**, 124; (b) S. Viviana, Biosens. Bioelectron., 2013, **47**, 12.

2 (a) C. Mathers, G. Stevens and M. Mascarenhas, Geneva, WHO, 2009; (b) A. Alwan, Geneva, WHO, 2011.

3 M. Nauck, W. H. Marz and Wieland, Clin. Chem., 2000, **46**, 436.

4 (a) C. P. Carvounis, S. Nisar and S. Guro-Razuman, Kidney I., 2002, **62**, 2223; (b) Rajesh, V. Bisht, W. Takashima and K. Kaneto, Biomaterials, 2005, **26**, 3683.

5 (a) Y. B. Hahn, R. Ahmad and N. Tripathy, Chem. Commun., 2012, **48**, 10369; (b) J. Wang, Chem. Rev., 2008, **108**, 814, (c) C. A. Rowe, S. B. Scruggs, M. J. Feldstein, J. P. Golden and F. . Ligler, Anal. Chem., 1999, **71**, 433; (d) N. Tripathy, R. Ahmad, E. Y. Kim, G. Khang and Y. B. Hahn, RSC Adv., 2014, **4**, 4604; (e) S. J. Pearton, T. Lele, Y. Tseng and F. Ren, Trends in Biotechnology, 2007, **25**, 481; (f) B. S. Kang, H. T. Wang, F. Ren, S. J. Pearton, T. E. Morey, D. M. Dennis, J. W. Johnson, P. Rajagopal, J. C. Roberts, E. L. Piner and K. J. Linthicum, Appl. Phys. Lett., 2007, **91**, 252103; (g) B. S. Kang, H. T. Wang, F. Ren and S. J. Pearton, Appl. Phys. Rev., 2008, **104**, 031101; (h) B. H. Chu, B. S. Kang, F. Ren, C. Y. Chang, Y. L. Wang, S. J. Pearton, A. V. Glushakov, D. M. Dennis, J. W. Johnson, P. Rajagopal, J. C. Roberts, E. L. Piner and K. J. Linthicum, Appl. Phys. Lett., 2008, **93**, 042114; (i) B. H. Chu, B. S. Kang, C. Y. Chang, F. Ren, A. Goh, A. Sciullo, W. Wu, J. Lin, B. P. Gila, S. J. Pearton, J. W. Johnson, E. L. Piner and K. J. Linthicum, IEEE Sensors Journal, 2010, **10**, 64.

6 (a) K. I. Chen, B. R. Li and Y. T. Chen, Nano Today Rev., 2011, **6**, 131; (b) H.-X. Ra, J.-T. Kim, R. Khan, D. Sharma, Y.-G. Yoon, Y.-B. Hahn, J.-H. Park, D.-G. Kim and Y.-H. Im, Nano Letters, 2012,**12**, 1891; (c) R. Ahmad, N. Tripathy, D. U. J. Jung and Y. B. Hahn, Chem. Commun., 2014, **50**, 1890; (d) O. S. Kwon, S. J. Park, J.-Y. Hong, A.-R. Han, J. S. Lee, J. S. Lee, J. H. Jang and J. Oh, ACS Nano, 2012, **6**, 1486.

7 (a) R. Ahmad, N. Tripathy, J.H., Kim and Y. B. Hahn, Sens. Actuators B, 2012, **174**, 195; (b) R. Ahmad, N. Tripathy and Y. B. Hahn, Biosens. Bioelectron., 2013, **45**, 281; (c) Yoon-Bong Hahn, Korean J. Chem. Eng., 2011, **28**, 1797.

8 (a) A. Qurashi, J. H. Kim, J. S. Lee and Y. B. Hahn, Electrochem. Commun., 2010, **12**, 475; (b) A. Qurashi, J. H. Kim and Y. B. Hahn, Electrochem. Commun., 2012, **18**, 88; (c) R. Ahmad, N. Tripathy, S. H. Kim, A. Umar, A. Al-Hajry and Y. B. Hahn, Electrochem. Commun., 2014, **38**, 4.

9 (a) Y.-K. Park, W.-Y. Rho, T. Mahmoudi and Y.-B. Hahn, Chem. Commun., 2014, **50**, 10502; (b) Y. Qin, X. Wang and Z. Wang, Nature, 2008, **451**, 809; (c) N. Tripathy, R. Ahmad, H. A. Ko, G. Khang and Y.-B. Hahn, Chem. Commun., 2015, **51**, 2585; (d) P. H. Yeh, Z. Li and Z. L. Wang, Adv. Mater., 2009, **21**, 4975; (e) Z. L., Wang and J. Song, Science, 2006, **312**, 242; (f) N. Tripathy, R. Ahmad, H. A. Ko, G. Khang and Y.-B. Hahn, Nanoscale, 2015, **7**, 4088; (g) C. Yang, C. Xu and X. Wang, Langmuir, 2012, **28**, 4580; (h) K. Byrappa, S. Ohara and T. Adschiri, Adv. Drug Delivery Rev., 2008, **60**, 299.

10 A. Rafiq, N. Tripathy and Y. B. Hahn, Sens. Actuators B, 2012, **169**, 382.

11 (a) E. S. Forzani, H. Zhang, L. A. Nagahara, I. Amlani, R. Tsui and N. Tao, Nano Letters, 2004, **4**, 1785; (b) M. Ahmad, C. Pan, Z. Luo and J. Zhu, J. Phys. Chem. C, 2010, **114**, 9308.

12 M. Ahmad, C. Pan, L. Gan, Z Nawaz and J. Zhu, J. Phys. Chem. C, 2010, **114**, 243.

13 R. K. Srivastava, S. Srivastava, T. N. Narayanan, B. D. Mahlotra, R. Vajtai, P. M. Ajayan and A. Srivastava, ACS Nano, 2012, **6**, 168.

